Geofísica Internacional (2003), Vol. 42, Num. 4, pp. 623-634

Overtides, compound tides, and tidal-residual current in Ensenada de la Paz lagoon, Baja California Sur, Mexico

José Gómez-Valdés[1], Juan A. Delgado[2] and Juan A. Dworak[2,3]
[1] *CICESE, Ensenada, Baja California, México*
[2] *Instituto Tecnológico del Mar 03, Guaymas, Sonora, México*
[3] *Centro de Investigaciones Biológicas del Noroeste, La Paz, Baja California Sur, México*

Received: May 24, 2001; accepted: October 28, 2002

RESUMEN

Se analizan las interacciones no lineales de la dinámica de marea en la laguna costera somera Ensenada de la Paz usando un modelo numérico bidimensional de las ecuaciones de la hidrodinámica verticalmente integradas. El modelo se calibra con observaciones de campo de mareas y de corrientes. Se corren dos experimentos para estudiar la influencia de diferentes parametrizaciones de la fricción del fondo. Los resultados indican que domina un balance entre el gradiente de presión y la fuerza de fricción del fondo en el área en estudio. MK_3, SK_3, MS_4 y M_4 resultaron las componentes de agua somera más energéticas. En el estudio estas ondas aparecen como resultado de la acción de los términos no lineales de la fricción del fondo, parametrizados según una ley cuadrática. Se encontró un patrón coherente de corriente residual inducida por marea. Dos giros anticiclónicos se generaron en el canal de entrada, los cuales se correlacionan con el patrón de flujo de energía de la onda M_4. En el interior de la laguna, en la parte más profunda, se generó un giro anticiclónico, el cual se correlaciona con los patrones de flujo de energía de las ondas M_2 y K_1; en cambio, en la parte más somera, se generó un giro ciclónico, el cual se correlaciona con la distribución del flujo de energía de la onda M_4.

PALABRAS CLAVE: Mareas, corrientes de marea, componentes de agua somera, corriente residual inducida por marea, modelo numérico, laguna costera, Golfo de California, Ensenada de la Paz.

ABSTRACT

Nonlinear tidal interactions in the shallow coastal lagoon Ensenada de la Paz, Mexico are investigated using a vertically-integrated two-dimensional numerical model. The model is calibrated with observations of sea surface elevation and currents. Two runs are implemented to study the role played by different bottom friction parameters. A dominant momentum balance between the pressure gradient force and the frictional force is found. MK_3, SK_3, MS_4, and M_4 were the most energetic shallow water tides. They are mainly generated by a quadratic bottom friction law. A coherent tide-induced residual current was found. Two anticyclonic eddies were generated at the inlet, they were correlated to the M_4 tidal energy flux. In the lagoon, in the deeper region, an anticyclonic eddy was generated, which was correlated with the M_2 and K_1 energy fluxes; but in the shallower region, a cyclonic eddy was generated, which was correlated with the M_4 energy flux.

KEY WORDS: Tides, tidal currents, shallow-water constituents, tidal-residual current, numerical model, coastal lagoon, Gulf of California, Ensenada de la Paz.

1. INTRODUCTION

The generation of overtides and compound tides is one of the dominant nonlinear physical processes in many coastal areas. It results from interactions between tidal flow and topography (Le Provost, 1991; Parker, 1991). Compound tides and overtides may produce flood/ebb asymmetries, which play an important role in the long-term distribution of sediments (Friedrichs and Aubrey, 1988). The tidal-residual flow in a coastal lagoon may also be induced by nonlinear interactions of tidal flow with topography. Because of the nonlinearity of these processes, numerical models are suitable to investigate the generation of shallow-water components and tidal residual flow (Le Provost and Fornerino, 1985; Werner and Lynch, 1987; Westerink *et al*., 1989; Davis and Jones, 1996).

From tide gauge observations, Godin and González (1991) found that the amplitudes of shallow-water tides are smaller than 2 cm along the West Coast of Mexico. Using a numerical model, Dworak and Gómez-Valdés (2003) (hereinafter DGV03) found that the shallow-water tidal currents are ~ 4 cm/s in Yavaros Bay, a coastal lagoon on the Gulf of California. Thus, to study the generation processes of this kind of waves on the West Coast of Mexico it is necessary to include the velocity field.

The Ensenada de La Paz (ELP) lagoon, located at 24°

08' N and 110° 22' W, is a shallow costal water body on the western coast of the Gulf of California. Sandoval and Gómez-Valdés (1997) (hereinafter SGV97) investigated the temporal and spatial variability of the flow in ELP. By using field measurements of sea surface elevation and horizontal currents over three periods of 29 days each, they documented the tidal flow and the low frequency flow in ELP. Their analysis of currents showed a rectilinear tidally induced flow, modified by ELP's geometry and friction. They also suggested nonlinear tidal waves in ELP. Godin (1983) analyzed a current record taken within the inlet of ELP. He found that the MS_4-current was ~2.5 cm/s. This figure is significant because SGV97 showed that the amplitude of the diurnal current is ~3 cm/s at neap tides. These field investigations on nonlinear tidal waves provide the data necessary to support a modeling investigation on generation of shallow-water tides in ELP.

The aim of this paper is to describe accurate simulations of the tidal motions in ELP, with special emphasis on the generation mechanisms of nonlinear tidal waves, with a two dimensional numerical model as a main tool. We extend the previous studies of this coastal lagoon to examine how the tidal-residual flow is generated. The basic role of quadratic friction on the nonlinear dynamics is demonstrated. The results should be of interest to hydrodynamic modelers using distribution of shallow-water constituents' considerations to determine tidal residual flow. The paper is organized as follows. Section 2 describes briefly the study area. In section 3 the mathematical model is presented. In section 4 the simulations of the main constituents are examined. In section 5, the shallow-water constituents are examined and in section 6 the residual flow is presented. Finally, in section 7 the paper concludes with a discussion of the tidal dynamics in coastal lagoon.

2. STUDY AREA

At the entrance to the Gulf of California the basic aspects of the local tides are well known (Godin *et al.*, 1980). M_2, K_1, S_2, and O_1 are the constituents of foremost importance. The ratio of $K_1 + O_1$ to $M_2 + S_2$ is close to 1 (Morales-Pérez and Gutiérrez, 1989), so the tides are of mixed type, mainly semidiurnal. This is a typical feature of tides within the Eastern Pacific. At ELP, which is the focus of this study, the tides cooscillate with the tides of the Gulf of California. Figure 1 shows the location of the study area. Although the emphasis of this study is on numerical experiments, the locations of instruments over the lagoon in previous studies are maintained as reference.

ELP is connected to Bahía de la Paz through an inlet 1.2 km wide, 4 km long and 7 m deep on average. The Bahía de la Paz is a bay with depths ranging from 300 m at the entrance to the bay to 10 m at the head. ELP has two distinctive topographic features, which we call the lagoon and the inlet. The lagoon is shallower than the inlet, with depths ranging from 2 to 6 m. At mean sea level, the surface area of ELP is approximately 45 km^2. The average tidal prism between low tide and the next high tide is approximately $50x10^6$ m^3. Morales and Cabrera-Muro (1982) estimated a flushing rate of $31x10^6$ m^3 per tidal cycle and the flushing time as 3.5 tidal cycles. The climate in the study area is semiarid, with an average annual rainfall of 200 mm.

To support our hypothesis, we carried out a cross-spectral analysis of the available measurements of sea level and currents in ELP to search for the importance of the high-frequency bands. Figure 2 shows the power spectral density of the currents relative to the semidiurnal values from the third-diurnal to the sixth-diurnal bands. To get those values we first calculated the variance in each band at A, B, and E moorings, then we divided the value of the power spectral density in each band by the corresponding semidiurnal variance. At the lagoon (E mooring) the relative variance of these bands is high, in agreement with the SGV97's suggestions.

3. MODEL

Tidal dynamics were simulated in ELP with a numerical model that uses the vertically-integrated equations of motion and the continuity equation, following Pritchard (1971), i.e.,

$$\frac{\partial u}{\partial t} + u\frac{\partial u}{\partial x} + v\frac{\partial u}{\partial y} + fv = -g\frac{\partial \eta}{\partial x} - k\frac{\sqrt{u^2+v^2}}{(h+\eta)}u + A_H\nabla_H^2 u, \quad (1)$$

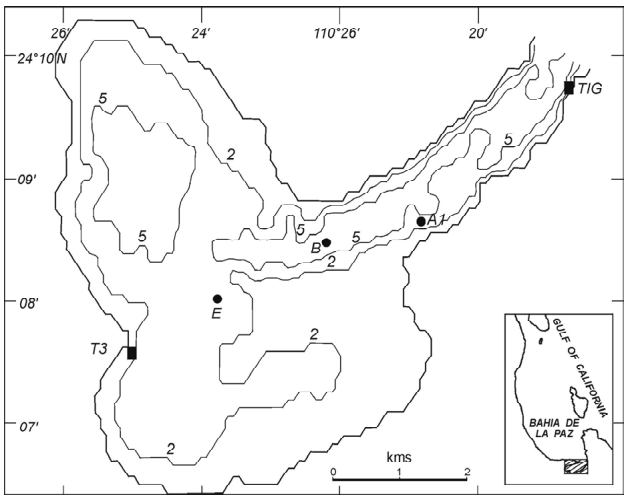

Fig. 1. Geographical location and bathymetry of the coastal lagoon Ensenada de La Paz, BCS, isobaths are in meters referred to mean sea level. ■ = tide gauges, ● = current meters.

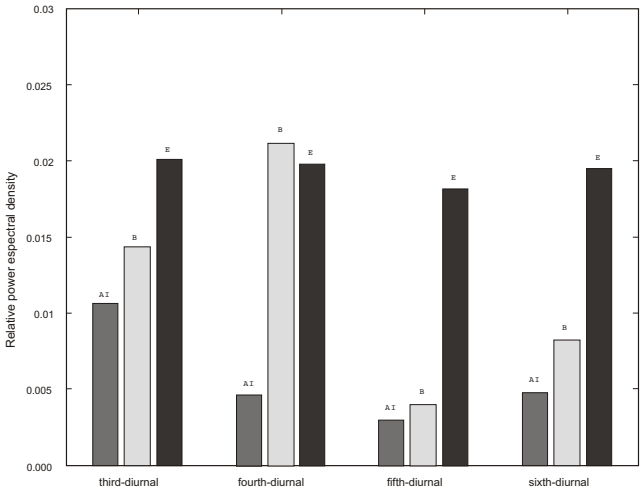

Fig. 2. Power spectral density of the third-, fourth-, fifth-, and sixth-diurnal band relative to semidiurnal variance.

$$\frac{\partial v}{\partial t} + u\frac{\partial v}{\partial x} + v\frac{\partial v}{\partial y} - fu = -g\frac{\partial \eta}{\partial y} - k\frac{\sqrt{u^2+v^2}}{(h+\eta)}v + A_H\nabla_H^2 v, \tag{2}$$

$$\frac{\partial \eta}{\partial t} + \frac{\partial\left[(h+\eta)u\right]}{\partial x} + \frac{\partial\left[(h+\eta)v\right]}{\partial y} = 0\ , \tag{3}$$

where $u(x,y,t)$ and $v(x,y,t)$ are the vertically-integrated velocities in the x and y directions respectively, t is the time, f is the Coriolis parameter, $\eta(x,y,t)$ is the sea surface elevation, $h(x,y)$ is the depth, and g is the acceleration due to gravity. Moreover, k represents a drag coefficient equal to gC_H^{-2}, where C_H is the Chézy coefficient, A_H is the horizontal eddy coefficient, and Δ_H is the horizontal Laplacian operator.

The boundary conditions are as follows. At the coast, the normal flow is zero and at the open boundary the model is driven by a tidal forcing $\eta_0(t)$, through the pressure gradient terms in the equations of motion as

$$\eta_0(t) = \sum_i A_i \cos(\omega_i t + \theta_i)\ , \tag{4}$$

where A_i, ω_i, and θ_i are the amplitudes, angular frequency, and phase of the i-th component. We used this kind of boundary condition because a very accurate $\eta_0(t)$ evolution can be supplied off the mouth of the lagoon, referring to previous studies of Godin *et al*. (1980).

Calculations are performed using the explicit method of finite differences on a staggered C-grid. The time evolution is computed with a leapfrog scheme. The time step is limited by the Courant Friedrich-Lewis's stability condition, which for the two-dimensional model is

$$\Delta t \le \frac{1}{\left[gh_{\max}\left(\frac{1}{\Delta x^2 + \Delta y^2}\right)\right]^{1/2}}\ , \tag{5}$$

where h_{max} is the maximum depth with reference to mean sea level (Wang, 1982), Δx and Δy are the grid sizes in the x and y direction respectively. The current version of the model does not incorporate mechanisms to handle drying and inundation. The numerical model has been used successfully to simulate tidal dynamics in Yavaros Bay (DGV03). The model was calibrated adjusting a set of k values until computed sea surface elevations and current tidal ellipses match the field values.

For computational reasons, the numerical grid had 106 *x* 63 points covering depths greater than 1m with respect to mean sea level to avoid cavitations and shock formation. The grid size was Δx = 123.76 m and Δy = 123.76 m. To maintain numerical stability, a time interval was Δt = 5 s. The horizontal eddy viscosity was $AH = 10^{-2}$ m^2/s that had been successfully used for a coastal lagoon in the Gulf of California (DGV03). The location of the open boundary was near the TIG (La Paz) tidal station, which is permanent. Table 1 shows the amplitudes of the tidal constituents used as boundary conditions. These values were obtained by interpolation between the TIG tidal station and Guaycura tidal station located in the Bahía de la Paz (Sandoval, 1983).

3.1 Calibration

The model was spun up from a state of rest ($\eta = 0$, (u, v)= 0). The model was run for 31 days and was calibrated against time series of the observed tidal harmonics from available stations as described next. From the model output, time series of surface elevations and velocity components were recorded hourly at each point of the domain, after four semidiurnal periods to avoid initial transients. Tidal harmonic analysis of the 29-day time series was performed to obtain the amplitude and phase of the sea surface elevation field and tidal current at each mesh point. In order to calibrate the model, we executed several computer runs, forcing the model with a linear combination of the astronomical and shallow-water constituents shown in Table 1. The inclusion of shallow-water constituents as boundary conditions at the open boundary allowed the propagation of these tides through the entrance (see also Tee, 1977). Two control points for sea surface elevation were set on the mesh points at the coordinates of the TIG and T3 stations and one control point for currents was set at the coordinates of the A1 mooring. A drag coefficient k = 3.5 x 10^{-3} brings the best agreement between the observed and predicted values. This result is in agreement with more elaborated depth dependent formulations of the bottom drag coefficient, such us that used for the San Francisco bay (Cheng *et al.*, 1993) and for the Yavaros Bay

Table 1

Amplitude (A) and phase (θ) values of the ocean boundary forcing for the main tidal constituents. Phase angles are referred to GMT. Time zone Z=+7.

	T(hr)	A(cm)	θ (°)
M_{sf}	354.3717	0.3	44
O_1	25.8193	20.1	188
K_1	23.9345	27.4	182
M_2	12.4206	22.7	114
S_2	12.0000	17.7	121
N_2	12.6584	4.8	110
SO_3	8.1924	1.3	246
MK_3	8.1771	0.8	245
SK_3	7.9927	0.7	230
M_4	6.2103	0.3	87
MS_4	6.1033	0.4	172
M_6	4.1402	0.1	56
$2MS_6$	4.0924	0.1	53
$2SM_6$	4.0456	0.1	68

Table 2

Phase shift (degrees) observed ($\delta\theta_{obs}$) and modeled ($\delta\theta_{mod}$) for the principal tidal constituents between the TIG and T3 tidal station, *u* and *v* velocity components (cm/s) observed (u_{obs},v_{obs}) and modeled (u_{mod},v_{mod}).

Tidal wave	$\delta\theta_{obs}$	$\delta\theta_{mod}$	u_{obs},v_{obs}	u_{mod},v_{mod}
O_1	5	4	8.81,3.1	9.6,2.8
K_1	8	7	13.6,3.3	14.5,4.3
M_2	16	17	30.8,7.5	30.6,8.1
S_2	16	15	27.8,6.8	26.9,6.5

(DGV03). Table 2 shows the modeled and observed phase shift between TIG and T3 and *u* and *v* velocity components at mooring A1. It follows that the 2-D model was successfully calibrated and that it provides reliable values. In the next two sections results from the numerical experiments after calibration are presented to examine the tidal flows.

4. THE M_2 AND K_1 TIDES

Sea surface elevations and horizontal velocity field were simulated for the main astronomical tides. Because of the similarity of the spatial distributions of the diurnal and semidiurnal components, we only present cotidal charts for the M_2 tide. The parameter's values on the maps are functions of the geographical locations. The amplitude of the M_2 tide (Figure 3 (a)) increases towards the head from the forced open boundary, in agreement with field observations. There is amplification close to 1 cm, attributable to basin configuration and friction (SGV97). In the lagoon the amplitude is almost the same everywhere. The phase lag varies more within the inlet than in the rest of the ELP because of the development of a strong frictional force there. The modeled phase shift between the mouth and the head was 17° (35 min), very close to the observed phase shift.The spatial distribution of the major and minor axis of the M_2 tidal current ellipse is shown at every other point of the numerical grid. The current ellipse distribution for the semidiurnal tides (Figure 3 (b)) showed a region of strong rectilinear flow (37 cm/s) at the inlet with the major axis aligned along the main channel. In the rest of the lagoon, the semi-major axes are aligned with topography, their magnitude decreases from the inlet to the lagoon due to continuity and shoaling. The spatial distributions of the tidal current ellipses for the rest of the semidiurnal and for the diurnal tides are similar to that found for the M_2, although with a reduced magnitude, e.g. the maximum speed for the K_1 is 22 cm/s.

Following Davis and Kwong (2000) we calculated tidal energy flux vectors over the ELP to study the relative magnitude of the tidal constituents. Figure 4 (a) shows the energy flux vectors of the M_2 tide. At the entrance the energy flux is high (a maximum of 60.8 KW/m) and rectilinear. In the lagoon the energy flux spreads out following topography, and it is clearly reduced due to shoaling. A cyclonic eddy is established at the NW region, which is correlated with a hole in the topography. The spatial distribution of tidal energy flux for the K_1 tide (Figure 4(b)) is similar to that found for the M_2, although with a reduced magnitude, e.g. the maximum energy flux for the K_1 tide is 25.8 KW/m. The cyclonic eddy was not present in the spatial distributions of energy flux of the S_2 and O_1 tides (not shown).

5. TIDAL ENERGY FLUX OF THE SHALLOW-WATER CONSTITUENTS

To gain additional insight into the nature of the tides in the ELP, we now present the results of the nonlinear interactions. The presence of overtides and compound tides are usually attributed to nonlinearities inherent to shallow water conditions. Overtides have periods that are an exact multiple of the fundamental constituents, e.g. M_4, a multiple of M_2, has a period of 6.21 hrs. Compound tides are linear combinations of two or more constituents, e.g. MS_4, a fourth-diurnal harmonic, whose period is 6.1035 hrs, arises from M_2 and S_2 interactions. Overtides and compound tides are detectable in the sea surface elevation and in the velocity fields (Le Provost, 1991; Parker, 1991; Aubrey and Speer, 1985).

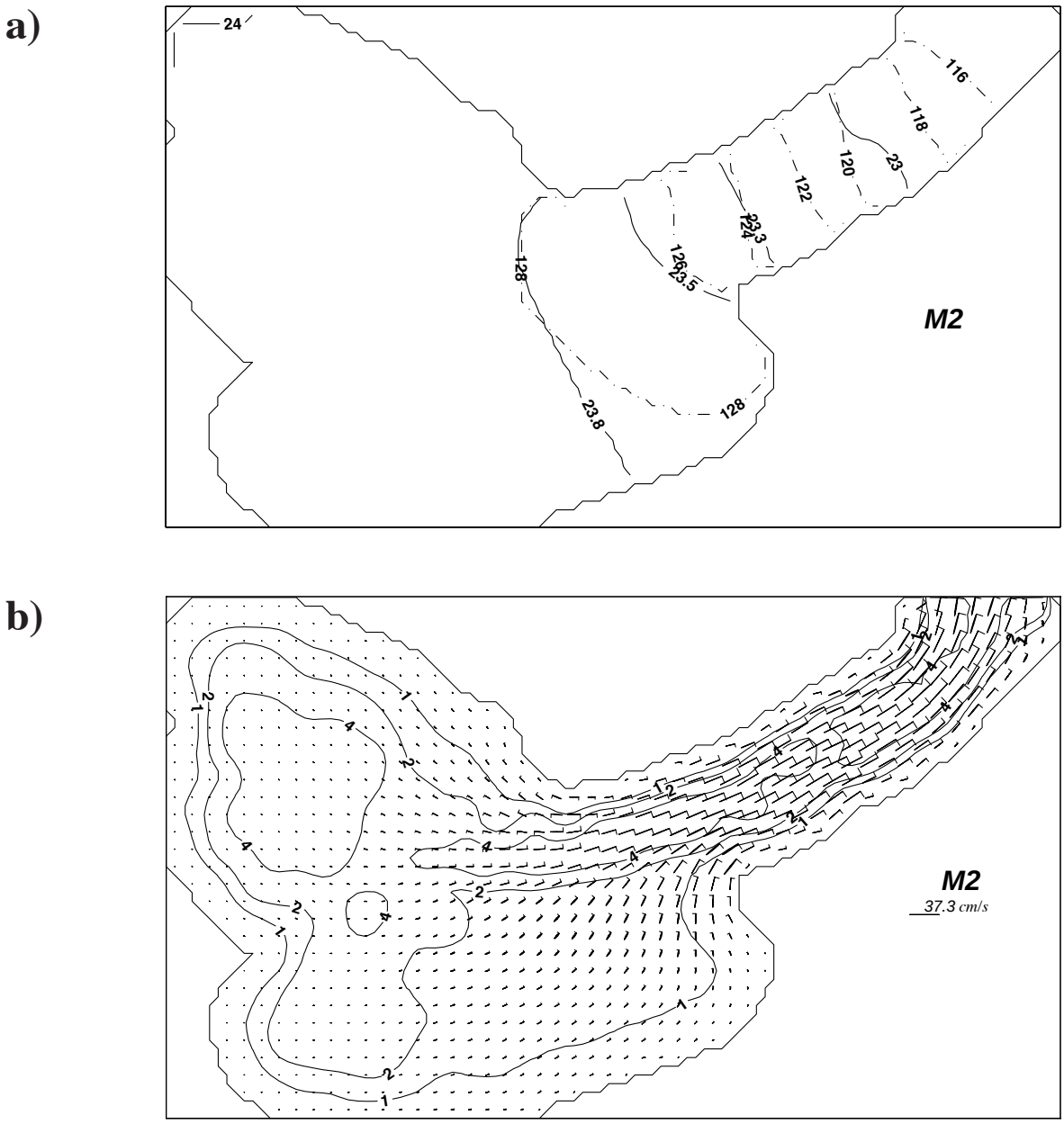

Fig. 3. (a) Computed amplitudes (solid lines, cm) and phases (dotted lines, deg) of surface elevation for the semidiurnal M_2 tide. Phases are referred to Greenwich. (b) Computed tidal current ellipses for M_2. Ellipses are depicted at every other point of the numerical grid. The line at the upper part of the ellipses shows the direction of rotation.

In this section, we now address the dynamics of the nonlinear waves at ELP.

By using the nonlinear tidal numerical model, we examined in detail the extent to which various nonlinearities generate the shallow-water tidal waves in addition to the degree to which the various nonlinear constituents affect each other. The spectra of overtides and compound tides were generated by forcing the numerical model with the linear combination of the tidal waves shown in Table 1. Several shallow-water constituents were generated in our experiments, which were resolved according to the Rayleigh's separation equation $(T|\sigma_2-\sigma_1|)>R$, where, σ_2 ,σ_1 are constituents frequencies, T is the record length, and R is the Rayleigh's constant (Godin, 1972). Components MK_3, SK_3, MS_4, and M_4 were resolved with the highest signal to noise ratio of all of the shallow-water tides.

We made maps of sea surface elevation, tidal current ellipses, and tidal energy flux vectors for the shallow-water

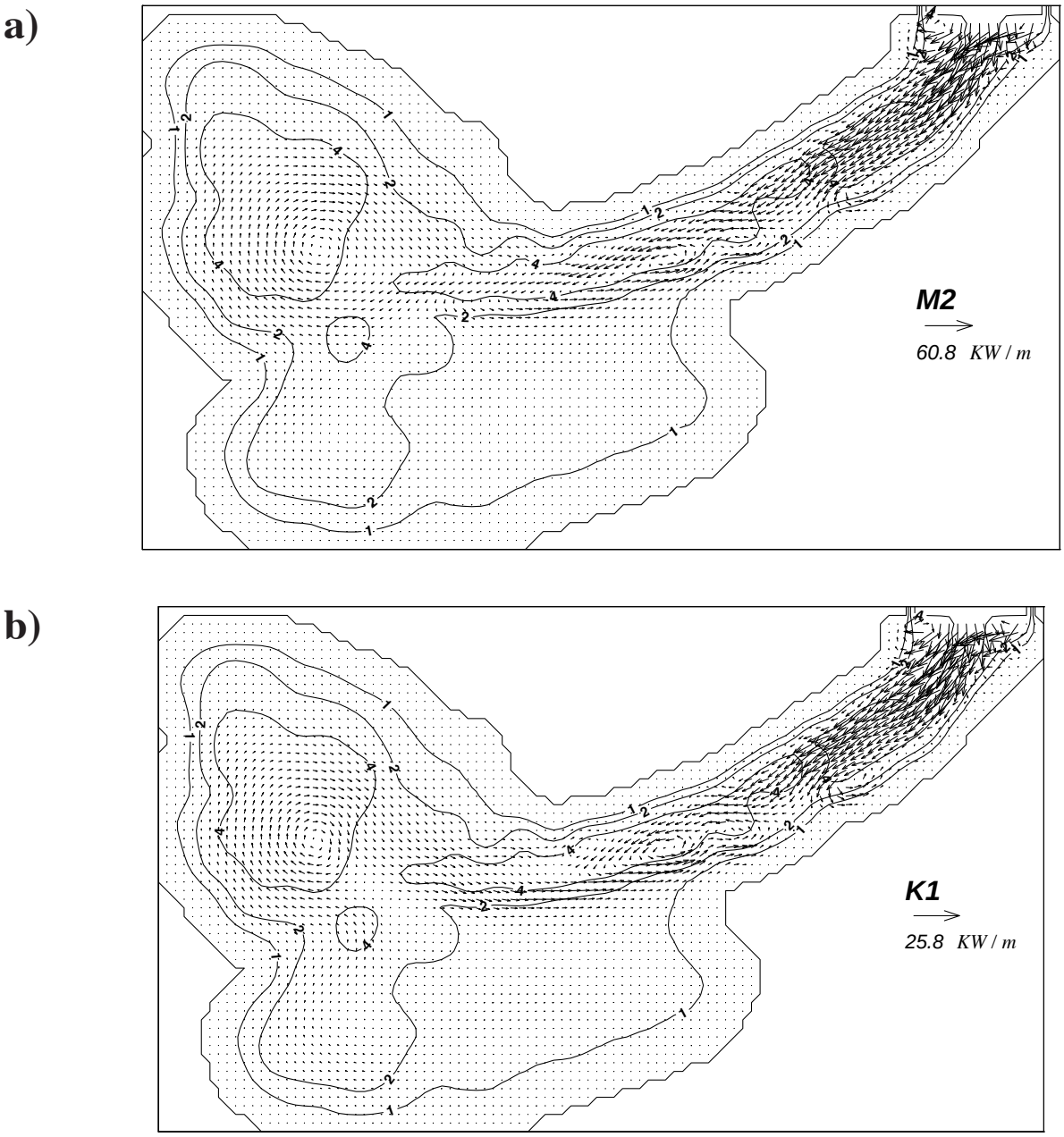

Fig. 4. Tidal energy flux for (a) the M_2 tide, and (b) the K_1 tide. The value represents the maximum energy flux.

tides. Because the later parameter includes both the sea surface elevation and currents information we present only maps of it. The distributions of MK_3 (Figure 5(a)) tidal energy flux vectors shows that the maximum energy flux out of the region (5.7 KW/m) occurs at the inlet, where the tidal velocity is stronger. Over the lagoon the area of minimum flux is confined to the shallow regions with low velocity. The spatial distribution of the SK_3 tidal energy flux (Figure 5(b)) is similar to that found for the MK_3 tide, but with a reduced magnitude. Figure 6 (a) shows that the main features of the MS_4 energy flux are comparable to those found for MK_3 and SK_3, although the magnitude of the energy flux is reduced. The distributions of M_4 tidal energy flux (Figure 6 (b)) shows two eddies at the inlet and one at the lagoon, while the magnitude of the energy flux is significantly smaller than in the case of MK_3, SK_3, and MS_4 tides.

Following DGV03 the mechanisms of generation of shallow-water constituents were investigated by comparison the mean quadratic values of the semi-major axis over the domain between the model output with a linear friction law and the model output with a quadratic friction law. Table 3

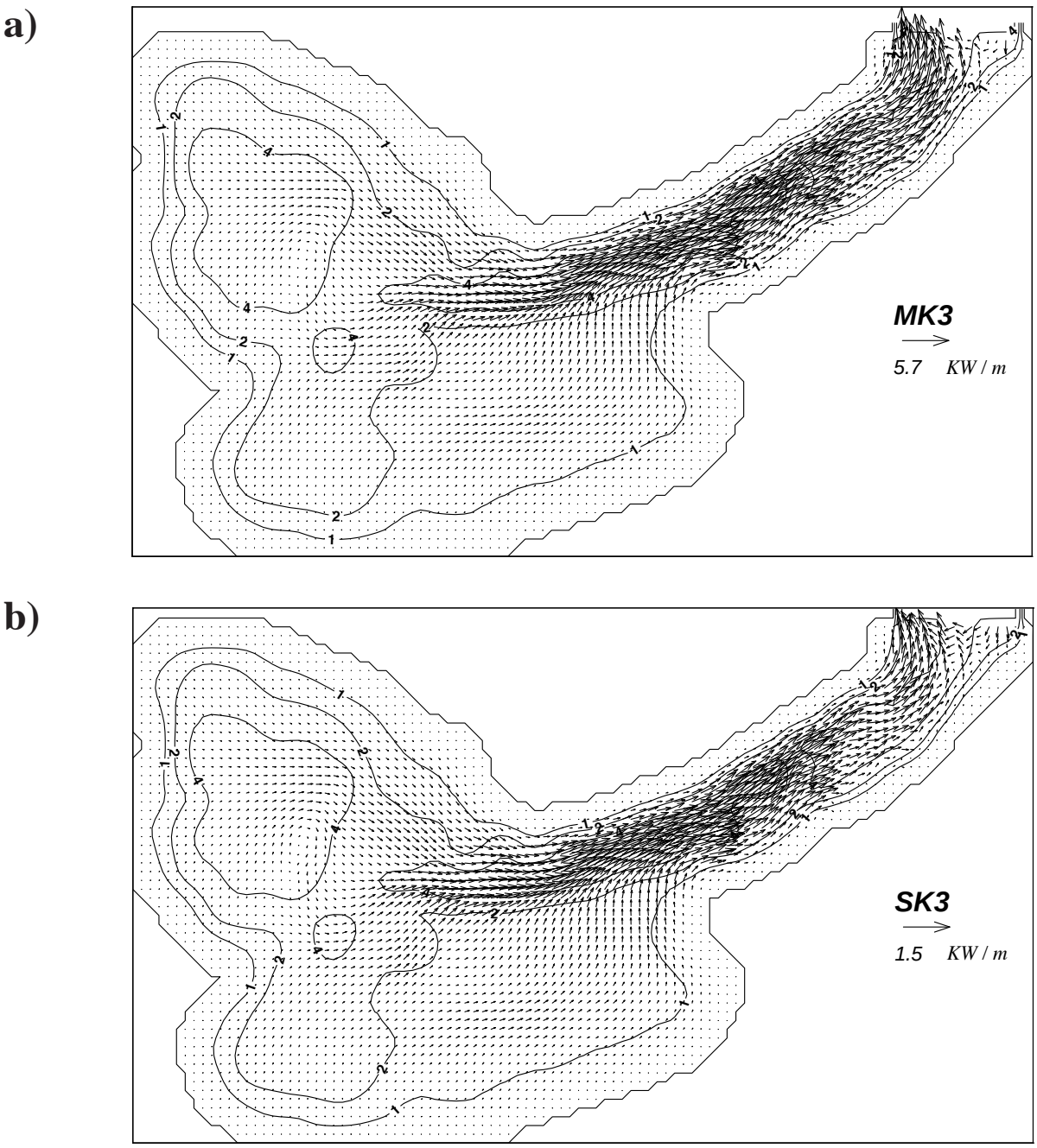

Fig. 5. As for Fig. 4, but for (a) the MK_3 tide and (b) the SK_3 tide.

shows that the nonlinear bottom friction term was the most important mechanism in the generation of shallow-water tides and also that the third-diurnal constituents were the strongest. In order to test the generation of shallow-water tides in the lagoon, we also ran the numerical model without shallow-water tides as boundary conditions as with those of Table 1. The amplitude patterns did not change significantly by using these boundary conditions as with those of Table 1.

In order to understand the relation between the length scale of the topographic features and the length scale of the motion, it is instructive to plot the tidal excursion length [$E = (uT/\pi)$, where u is the velocity and T is the period]. Figure 7(a) shows the tidal excursion of M_2 tide and M_4 over the ELP. At the inlet, the tidal excursion of M_2 is between 1.9 and 4.6 km, while the tidal excursion of M_4 is between 0.5 and 0.8 km. At the lagoon, the tidal excursion of M_2 is about 0.5 km, while the tidal excursion of M_4 is about 0.1 km.

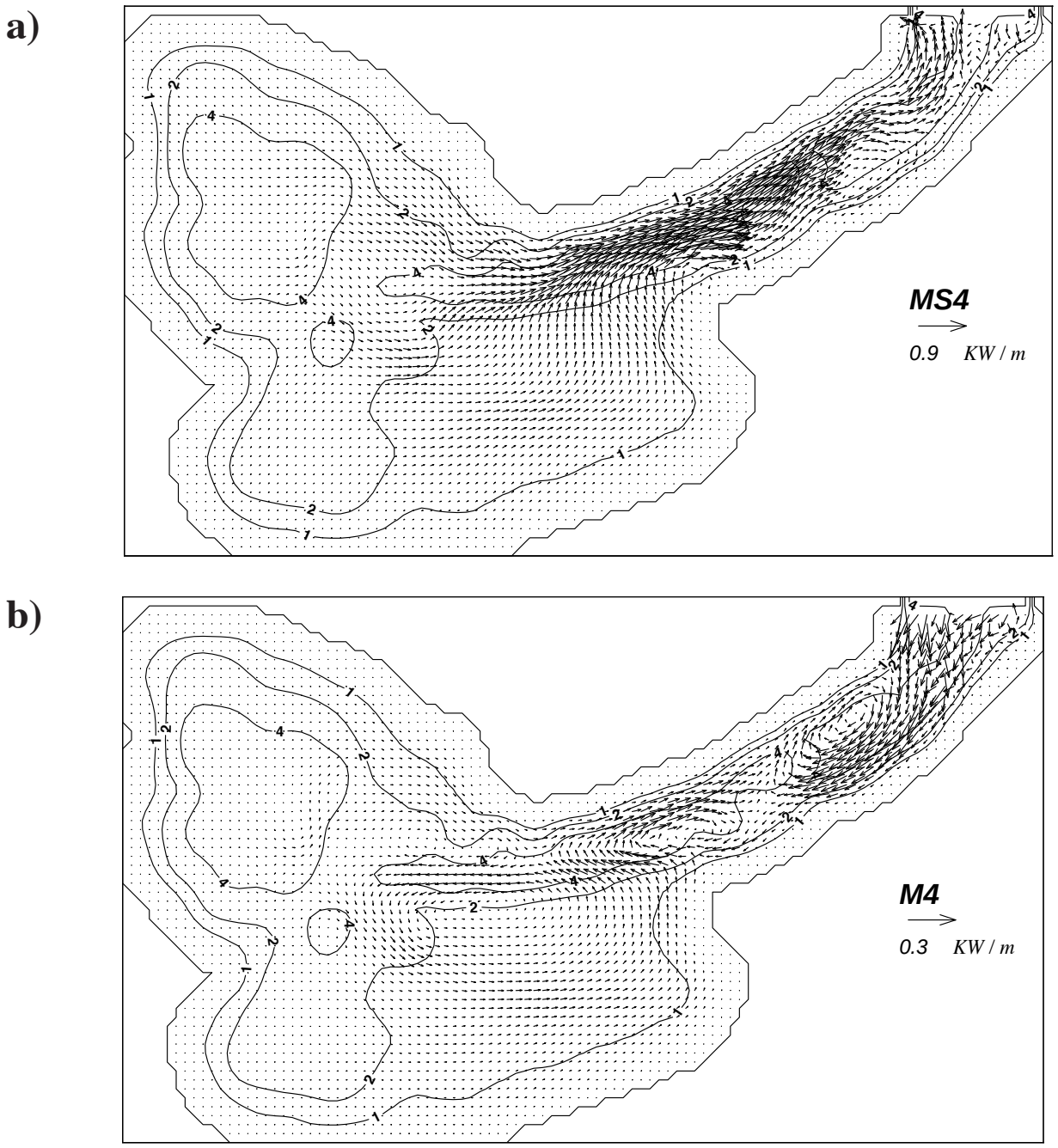

Fig. 6. As for Fig. 4, but for (a) the MS_4 tide and (b) the M_4 tide.

6. RESIDUAL CURRENT

The tide-induced residual flow can be estimated from the mean (Z_0) of the harmonic analysis. As the tide-induced residual flow is derived as the averaged flow generated by the nonlinearity of the tidal currents, Z_0 provides a good estimate (Parker, 1991). Figure 7 (b) shows the distribution of Z_0 at ELP for the nonlinear model forced by the multiple tidal constituents, whose amplitude values are shown in Table 1. The maximum velocity (7.4 cm/s) occurs at the inlet, where two anticyclonic eddies are set. In addition, two half-basin scale eddies, one with anticyclonic rotation and the other one with cyclonic rotation, take place at the lagoon, whose are correlated with topography.

7. DISCUSSION AND CONCLUSIONS

A two-dimensional vertically-integrated model is useful for prediction of sea level and barotropic tidal currents in a coastal lagoon. It can also be used for studies of generation

a)

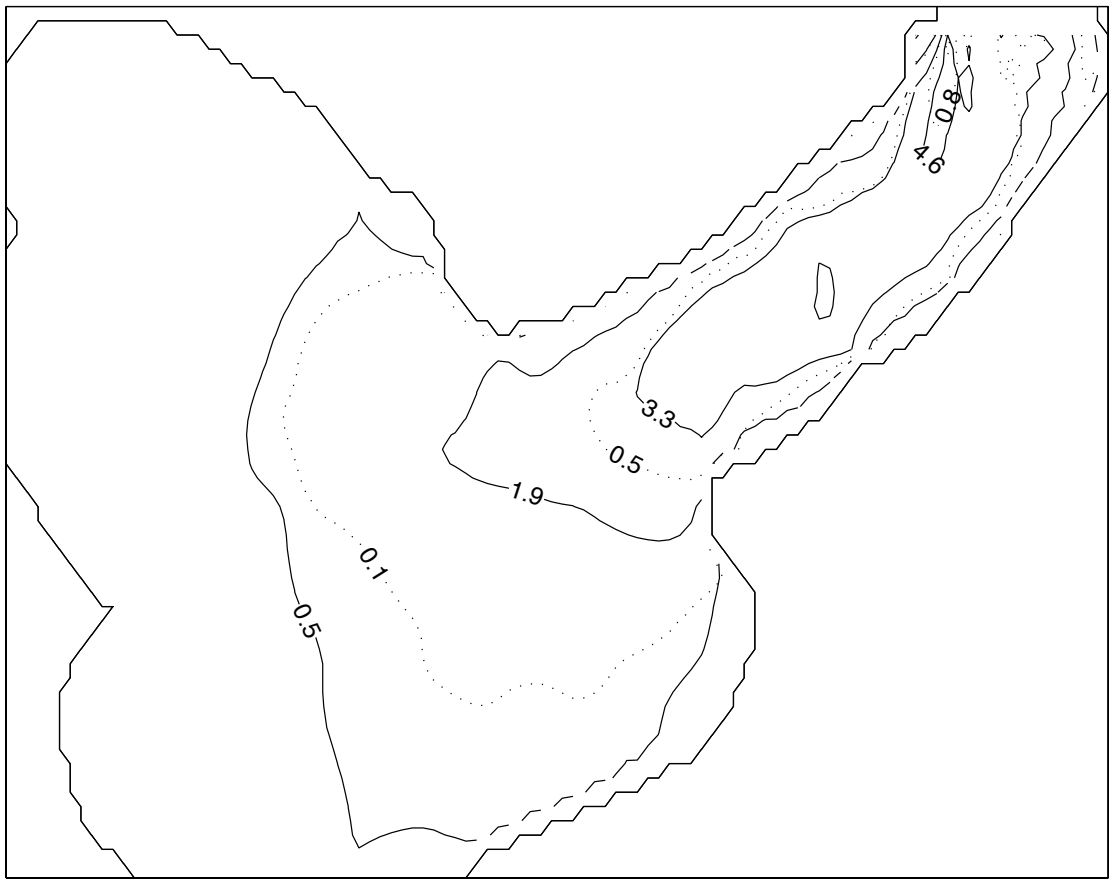

b)

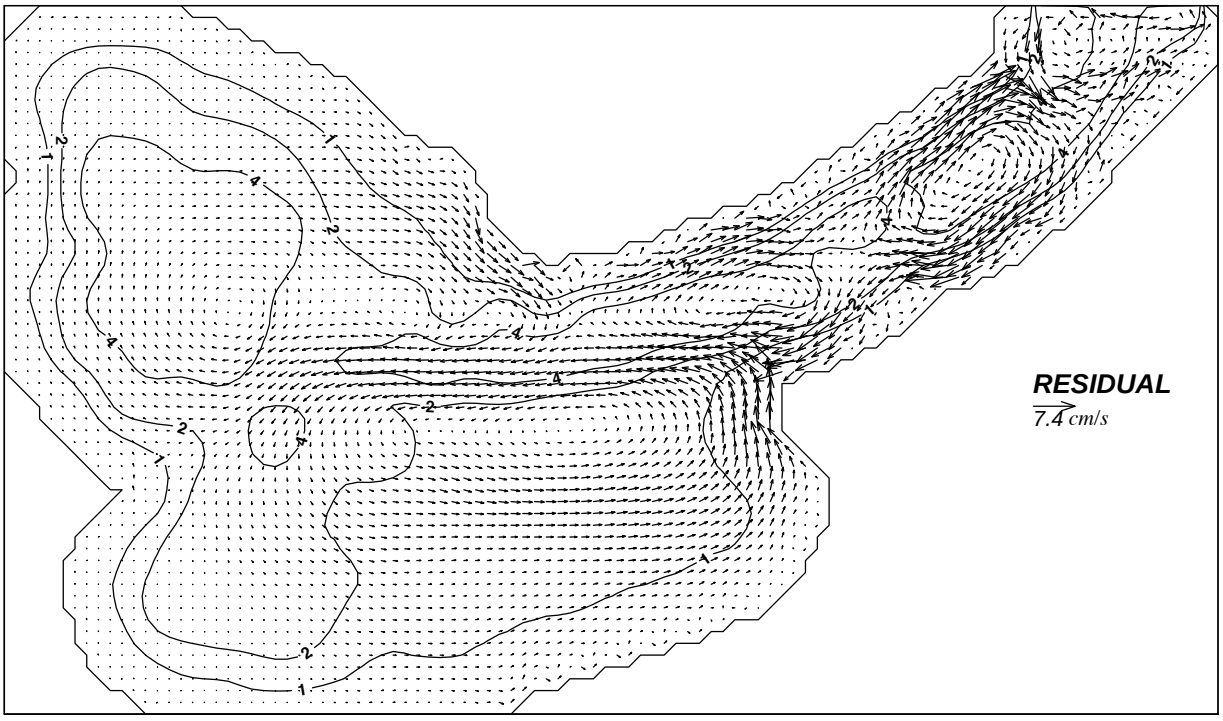

Fig. 7. (a) Tidal excursion in km. Continuous line for M_2 and dotted line for M_4. (b) Tidal residual current (Z0) in cm/s.

Table 3

Comparison of mean quadratic values of semi-major axis over the domain between the model output with quadratic friction and linear friction for the shallow-water constituents.

Constituents	T(hr)	$\langle M^2 \rangle \times 10^{-2}$ ($cm^2\ s^{-2}$) Quadratic Friction	$\langle M^2 \rangle \times 10^{-2}$ ($cm^2\ s^{-2}$) Linear Friction
MK_3	8.1771	926	46
SK_3	7.9927	282	9
M_4	6.2103	74	2
MS_4	6.1033	128	4
M_6	4.1402	10	0
$2SM_6$	4.0924	54	0

of overtides, compound tides, and residual tidal circulation. Our numerical experiments show the evolution of the tidal flow and its nonlinear interactions in the ELP by using a high-resolution grid.

The vertically-integrated dynamics associated to the diurnal and semidiurnal tides was simulated in good agreement with observations. The coefficient of friction was of the same order of magnitude to that obtained in other studies, e.g. Marinone (1997) in a numerical tidal study on the Gulf of California found a $k = 4.4x10^{-3}$. The calculated tidal flow is rectilinear in the inlet and rotary in the inner basin, in agreement with previous studies on tides in Ensenada de la Paz (Morales and Cabrera-Muro, 1982; Granados-Guzmán and Álvarez-Borrego, 1984; SGV97). Therefore, our numerical model is suitable to investigate the generation of overtides, compound tides, and tidal-residual current (Z_0).

The strength of the compound tides depends on the energy level from which they are formed (Speer and Aubrey, 1985). Previous studies on generation of shallow-water components have mostly been undertaken in coastal environments where the tidal regime is predominantly semidiurnal (Aubrey and Speer, 1985; Le Provost, 1991; Sinha and Pingree, 1997). However, in ELP the tidal regime is mixed, mainly semidiurnal, so almost all the spectrum of the shallow- water constituents is generated there. Because M_2 and K_1 are the most energetic waves, our model showed that any linear combination among them was generated in the ELP. MK_3, SK_3, MS_4, and M_4 were the most energetic shallow-water tides. To plot tidal energy flux vectors of each constituent was a very useful tool to study the importance of the shallow-water tides. By keeping the nonlinear terms of advection and continuity in both a model with a linear friction law and a model with a quadratic friction law, we found that the amplitude of the shallow-water tides reach the highest amplitudes by the action of the later mechanism. A different approach is discussed in (Pingree and Maddock, 1978)

The tide-induced residual flow was inferred from the Z_0 component of the harmonic analysis of current series. Tidal residual flow is essentially a rotational motion that forms eddies (Yanagi, 1999). The classical eddy-structure in inlet/lagoon systems (Murty *et al*., 1980) was found in the ELP. Two anticyclonic eddies were generated at the inlet, whose were also found in the tidal energy flux pattern of the M_4 tide. At the lagoon, in the deeper region, an anticyclonic eddy was generated, which was also found in the tidal energy flux patterns of the M_2 and K_1 tides. However, in the shallower region, a cyclonic eddy was generated, which was also found in the tidal energy flux pattern of the M_4 tide. The observations reported by Morales and Cabrera Muro (1982) and SGV97 are consistent with these features. The equivalence of the tidal residual pattern with the tidal energy flux pattern indicates that bottom friction is the main mechanism that regulates both processes. The maximum tidal residual vorticity is expected when the topographic length scale is the order of the tidal excursion length (Zimmerman, 1981). The size of the inlet is the same order than the tidal excursion length of the M_2 tide, the strongest astronomical tide. Furthermore, the size of the hole at the lagoon (~ 1 km) is two times the tidal excursion length of M_2 and this ratio is also suitable for the maximum response (Park and Wang, 1994).

ACKNOWLEDGMENTS

The observational program was performed under grants by SEP, CONACyT-SIMAC (grant # 990107018), Mexico. We wish to thank Eduardo Morales, Felipe Plaza, Homero Cabrera and Salvador Farreras for helping us on the cruises. A. Valle-Levinson, S.G. Marinone, J. L. Ochoa and Oscar U. Velasco Fuentes provided helpful suggestions to an early version of this manuscript. J. M. Domínguez helped us to draw Figure 1. L. E. Elenes helped us to solve electronic troubles. The final version of this manuscript was worked out while J. Gómez-Valdés was a visiting scholar at Scripps Institution of Oceanography.

BIBLIOGRAPHY

AUBREY, D. G. and P. E. SPEER, 1985. A study of non-linear tidal propagation in shallow inlet/estuarine systems Part I: Observations. *Estuarine, Coastal and Shelf Sci. 21,* 185-205.

CHENG, R. T., V. CASULLI and J. W. GARTNER, 1993. Tidal, Residual and Intertidal Mudflat (TRIM) model

and its applications to San Francisco Bay, California. *Estuarine, Coastal and Shelf Sci. 36,* 235-280.

DAVIS, A. M. and J. E. JONES, 1996. Sensitivity of tidal bed stress distributions, nearbed currents, overtides, and tidal residuals to frictional effects in the Eastern Irish Sea. *J. Phys. Oceanogr. 26,* 2553-2575.

DAVIS, A. M. and S. C. KWONG, 2000. Tidal energy fluxes and dissipation on the European continental shelf. *J. Geophys. Res., 105,* 21 969-21 989.

DWORAK, A. J. and J. GÓMEZ-VALDÉS, 2003. Tide-induced residual current in a coastal lagoon of the Gulf of California. *Estuarine, Coastal and Shelf Sci. 57,* 99-109.

FRIEDRICHS, C. T. and D. G. AUBREY, 1988. Nonlinear tidal distortion in shallow-water mixed estuaries. A synthesis. *Estuarine, Coastal and Shelf Sci. 27,* 521-545.

GODIN, G., 1972. The analysis of tides. University of Toronto Press. Toronto. 264 pp.

GODIN, G., N. DE LA PAZ RODRÍGUEZ and M. ORTIZ, 1980. La marea y el nivel del mar a lo largo de la costa occidental de México. *Geofís. Int. 19,* 239-258.

GODIN, G., 1983. The spectra of point measurements of currents: their features and their interpretation. *Atm.-Ocean 21,* 263-284.

GODIN, G. and I. GONZÁLEZ, 1991/92. About some very small harmonics which are present in the tide of the Pacific. *Deutsche Hydrographische Zeitschrift 44,* 115-132.

GRANADOS-GUZMÁN, A. and S. ÁLVAREZ-BORREGO, 1984. Variabilidad de temperatura en La Ensenada de La Paz B. C. S. *Cienc. Mar. 9,* 133-141.

LE PROVOST, C. and M. FORNERINO, 1985. Tidal spectroscopy of the English Channel with a numerical model. *J. Phys. Oceanogr. 15,* 1009-1031.

LE PROVOST, C., 1991. Generation of overtides and compound tides (review). *In:* Tidal hydrodynamics (Parker, B. B., ed.). John Wiley and Sons, New York, pp. 269-295.

MARINONE, S. G., 1997. Tidal residual currents in the Gulf of California: Is the M2 tidal constituent sufficient to induce them? *J. Geophys. Res. 102,* 8611-8623.

MORALES, G. R. and H. CABRERA-MURO, 1982. Aplicación de un modelo numérico unidimensional a La Ensenada de La Paz B. C. S. *Cienc. Mar. 8,* 69-89.

MORALES-PÉREZ, R. A. and G. GUTIÉRREZ, 1989. Mareas en el Golfo de California. *Geofís. Int. 28,* 25-46.

MURTY, T. S., F. G. BARBER and J. D. TAYLOR, 1980. Role of advective terms in tidally generated residual circulation. *Limnol. Oceanogr., 25,* 529-533.

PARK, M.-J. and D.-P. WANG, 1994. Tidal vorticity over isolated topographic features. *Cont. Shelf Res. 14,* 1583-1599.

PARKER, B. B., 1991. The relative importance of the various nonlinear mechanisms in a wide range of tidal interactions (review). *In:* Tidal hydrodynamics (Parker, B. B., ed.). John Wiley and Sons, New York, pp. 237-268.

PINGREE, R. D. and L. MADDOCK, 1978. The M_4 tide in the English Channel derived from a non-linear numerical model of the M_2 tide. *Deep Sea Res. 25,* 53-66.

PRITCHARD, D. W., 1971. Hydrodynamic Models. *In:* Estuarine modelling an assessment (Ward, Jr., G. H. and Espey, Jr., W. H., eds.). Water Quality Office, U.S. Environmental Protection Agency, pp. 5-33.

SANDOVAL, J. F., 1983 Análisis estadístico de la corriente de marea y la influencia del viento sobre la Ensenada de la Paz, BCS. B. Sci. Thesis, Escuela Superior de Cienc. Mar., Universidad Autónoma de Baja California. Ensenada, B. C., México. 118 pp.

SANDOVAL, J. F. and J. GÓMEZ-VALDÉS, 1997 Tides and tidal currents in Ensenada de la Paz lagoon, Baja California Sur, México. *Geofís. Int. 36,* 37-47.

SINHA, B. and R. D. PINGREE, 1997. The principal lunar semidiurnal tide and its harmonics: baseline solutions for M_2 and M_4 constituents on the North-West European Cont. Shelf. *Cont. Shelf Res. 17,* 1321-1365.

SPEER, P. E. and D. G. AUBREY, 1985. A study of nonlinear tidal propagation in shallow inlet/estuarine systems Part II: Theory. *Estuarine, Coastal Shelf Sci. 21,* 207-224.

TEE, K. T., 1977. Tide-induced residual current - Verification of a numerical model. *J. Phys. Oceanogr. 7,* 396-402.

WANG, D-P., 1982 Development of a three-dimensional, limited-area (island) shelf circulation model. *J. Phys. Oceanogr. 12,* 605-617.

WERNER, F. E. and D. R. LYNCH, 1987. Field verification of wave equation tidal\dynamics in the English Channel and Southern North Sea. *Adv. Water Resour. 5,* 115-129.

WESTERINK, J. J., K. D. STOLZENBACH and J. J. CONNOR, 1989. General spectral computations of the nonlinear shallow water tidal interactions within the Bight of Abaco. *J. Phys. Oceanogr. 9,* 1348-1371.

YANAGI, T., 1999. Coastal oceanography. Kluwer Academic Publishers, Boston, 162 pp.

ZIMMERMAN, Z. T. F., 1981. Dynamics, diffusion and geomorphological significance of tidal residual eddies. *Nature 290,* 549-555.

José Gómez-Valdés[1], Juan A. Delgado[2] and Juan A. Dworak[2,3]

[1] Centro de Investigación Científica y de Educación Superior de Ensenada (CICESE), Km 107, Carr. Tijuana-Ensenada, Ensenada, Baja California, México
Email: jgomez@cicese.mx
[2] Instituto Tecnológico del Mar 03, Km 4, Carr. al Varadero Nacional. Guaymas, Sonora. México.
[3] Centro de Investigaciones Biológicas del Noroeste, Km 1 a San Juan de la Costa, "El Comitán", La Paz, Baja California Sur, México.
Email: jdworak@cicese.mx